Amplitude analysis of $\pi^{\pm}$-^{12}C elastic scattering

H. G. Schlaile
Institut für Theoretische Teilchenphysik, Universität Karlsruhe, D-76128 Karlsruhe, Federal Republic of Germany
(Received 30 October 1996)

An energy-dependent amplitude analysis of $\pi^{\pm}$-^{12}C elastic-scattering data in the pion energy range from 486 to 870 MeV was carried out. Using a careful treatment of Coulomb effects to describe the Coulomb nuclear interference together with the constraints from the $\pi^{\pm}$-^{12}C forward amplitude f_0 by dispersion relations allows a stringent consistency check of the data. In general a satisfactory description of the data was achieved, but recent π^{-}-^{12}C elastic-scattering data need considerable normalization factors to fit into the framework. The still not measured π^{+}-^{12}C data as well as the $\pi^{\pm}$-^{12}C data at 870 MeV are predicted. Phase shifts are calculated by partial wave projection of the amplitudes. The partial waves are summed up to obtain the total, total-elastic and total-inelastic cross sections. [S0556-2813(97)07105-7]

PACS number(s): 25.80.Dj, 13.75.Gx, 24.10.−i

I. INTRODUCTION

Recently systematic measurements of π^- elastic scattering have been taken at 610, 710, 790, and 895 MeV/c by Takahashi *et al.* [1]. These data sets are systematically by 10–15% below the values taken by Marlow *et al.* [2]. This is also true for the total cross sections extracted from Ref. [1] compared with earlier data from Crozon *et al.* [3] and Clough *et al.* [4]. The purpose of the present work is to show how well the data can be fitted into the framework of an energy-dependent amplitude analysis including the constraints from forward dispersion relations. Within this framework a good representation of the measured data sets as well as predictions for the still not measured π^{+}-^{12}C elastic scattering can be given, taking into account normalization factors for the differential cross sections. Furthermore, the fit parameters have been extrapolated to 1 GeV/c where Takahashi *et al.* measured both π^- and π^+ elastic differential cross sections. The present analysis is performed along the lines of earlier works on $\pi^{\pm}$-^{4}He [6], $\pi^{\pm}$-^{12}C [7], $\pi^{\pm}$-^{16}O [8], and $\pi^{\pm}$-^{40}Ca [9]. In the analysis the forward dispersion relation is used as described in Ref. [10] to obtain the real part of the forward scattering amplitude from the imaginary part as given by the total cross section. In Sec. II a short description of the formalism used to treat the Coulomb effects is given, and Sec. III handles the dispersion relation, Sec. IV shows the hadronic amplitude, and in Sec. V we look on the results compared with the data from Refs. [1] and [2] and the total cross sections as measured during the past 30 years.

II. COULOMB CORRECTIONS

The elastic differential cross section of $\pi^{\pm}$-^{12}C scattering is described by

$$\frac{d\sigma^{\pm}}{d\Omega}=|f_{\rm tot}^{\pm}|^2. \tag{1}$$

The total amplitude $f_{\rm tot}^{\pm}$ consists of a sum of three parts

$$f_{\rm tot}^{\pm}=f_h+f_C^{\pm}+f_R^{\pm}, \tag{2}$$

f_h is the pure hadronic, $f_C^{\pm}$ the pure Coulomb amplitude, and $f_R^{\pm}$ represents the Coulomb corrections which take into account the modifications of the pure hadronic force by Coulomb effects. $f_C^{\pm}$ can be split into the part $f_C^{\rm point\pm}$, where the pion and the ^{12}C nucleus are treated as pointlike particles, and $f_C^{\rm ext\pm}$, which represents the contribution from the charge extension of $\pi^{\pm}$ and ^{12}C to the Coulomb amplitude [11]:

$$f_C^{\pm}=f_C^{\rm point\pm}+f_C^{\rm ext\pm}. \tag{3}$$

$f_C^{\rm ext\pm}$ is calculated numerically with the ^{12}C form factor F_C of Dumbrajs [12] and the pion form factor F_π of Bebek [13].

The differential cross section at very small scattering angles is sensitive to relativistic effects in the point Coulomb amplitude. We use the accurate formula [14,15]

$$f_C^{\rm point\pm}=f_C^{(0)}+f_C^{(1)}+\Delta f_C^{(1)}, \tag{4}$$

where

$$f_C^{(0)}=-\frac{\eta}{2k\,\sin^2\left(\frac{1}{2}\Theta\right)}\;e^{-i\eta\,\ln\,\sin^2(1/2\Theta)+2i\sigma_0}, \tag{5}$$

$$f_C^{(1)}=f_C^{(0)}\left[-\frac{1}{2}\;\pi\eta v_{\rm lab}^2\,\sin\left(\frac{1}{2}\Theta\right)e^{2i\sigma_{-1/2}+2i\sigma_0}\right], \tag{6}$$

$$\Delta f_C^{(1)}=-\sum_{l=0}^{L}\,f_{C,l}^{(1)}+\frac{1}{2ik}\sum_{l=0}^{L}\,(2l+1)\times(e^{2i\sigma_\gamma}-e^{2i\sigma_l})P_l(\cos\Theta). \tag{7}$$

TABLE I. Effective coupling constants from ^{4}He to ^{40}Ca.

Nucleus	$\omega_n\, f_{\rm eff}^2$ (MeV)	Reference
^{4}He	−6	[6]
^{12}C	−25	Present work
^{16}O	−37	[7]
^{40}Ca	−51	[6]

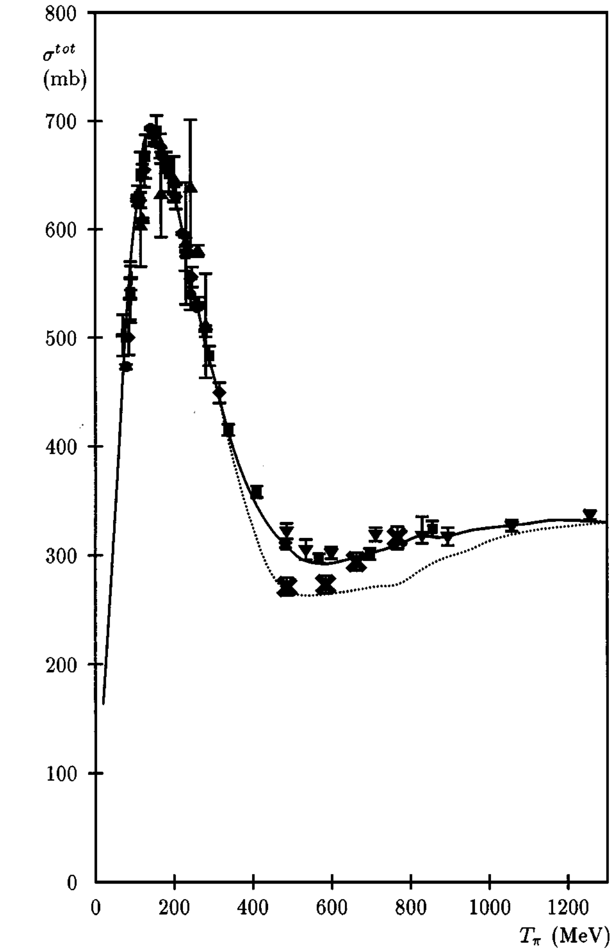

FIG. 1. Total cross section obtained from the fit. The data are from Wilkin *et al.* [18] ●, Mutchler [19] ○, Binon *et al.* [20] +, Das and Deo [21] △, Crozon *et al.* [3] ▽, Clough *et al.* [4] □, Ashery *et al.* [22] ◇, and Takahashi *et al.* [1] ×. The dotted line relies on the data of Takahashi *et al.* [1].

η is the Sommerfeld parameter, $\gamma=[(l+1/2)^2-Z^2\alpha^2]^{1/2}$ with $Z=6$ and $\alpha=1/137$. Θ is the scattering angle, $v_{\rm lab}$ the velocity of the pion, and L is the maximum angular momentum taken into account. $f^{(1)}_{C,l}$ is the partial wave decomposition of $f^{(1)}_C$ and $\Delta f^{(1)}_C$ replaces the approximate relativistic part of the Coulomb phase shift by the fully relativistic one [9] for partial waves up to $L=20$. The σ's are given by

$$e^{2i\sigma_{\bar{l}}}=\frac{\Gamma(\bar{l}+1+i\eta)}{\Gamma(\bar{l}+1-i\eta)}, \tag{8}$$

$$e^{2i\sigma_{\gamma}}=e^{-i\pi(\gamma-1/2-l)}\,\frac{\Gamma(\gamma+1/2+i\eta)}{\Gamma(\gamma+1/2-i\eta)}, \tag{9}$$

where $\bar{l}$ is either $-1/2$ (in $\sigma_{-1/2}$) or l.

The fact that negative pions are accelerated towards the nucleus while positive pions are slowed down changes not only the momentum of the pions but also their impact parameter. This is accounted for by the last contribution $f^{\pm}_R$ in

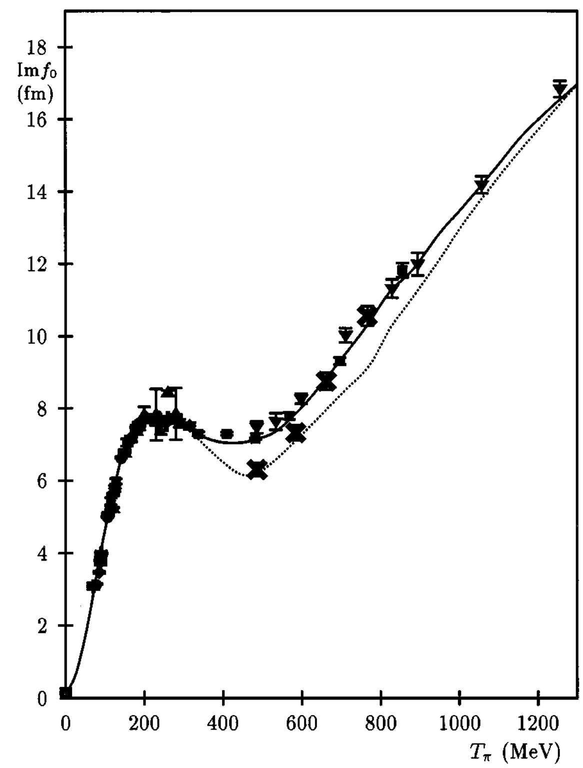

FIG. 2. Imaginary part of the forward amplitude. The data are from Wilkin *et al.* [18] ●, Mutchler *et al.* [19] ○, Binon *et al.* [20] +, Das and Deo [21] △, Crozon *et al.* [3] ▽, Clough *et al.* [4] □, Ashery *et al.* [22] ◇, and Takahashi *et al.* [1] ×, the dotted line relies on the data of Takahashi *et al.* [1].

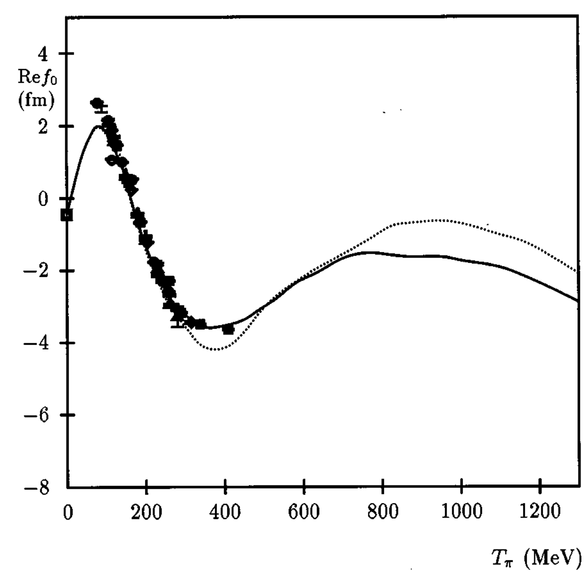

FIG. 3. Real part of the forward amplitude. The data are from Wilkin *et al.* [18] ●, Mutchler *et al.* [19] ○, Binon *et al.* [20] +, Das and Deo [21] △, Clough *et al.* [4] □, and Ashery *et al.* [22] ◇. In those cases, where no real parts had been given, the ratio real to imaginary part from Wilkin *et al.* had been adopted. The dotted line relies on the data of Takahashi *et al.* [1].

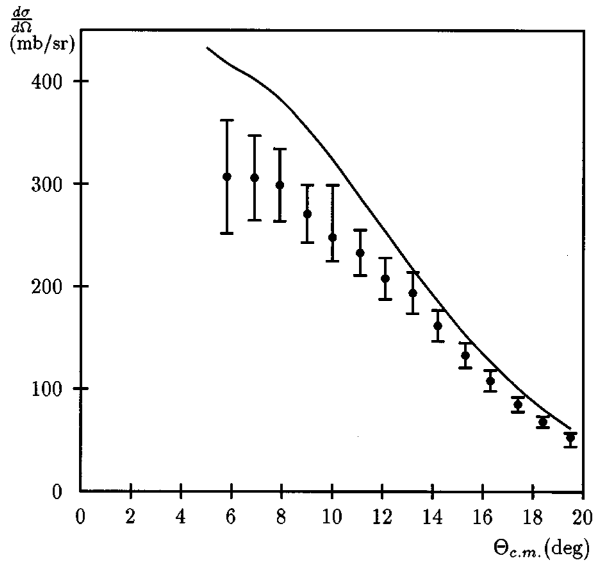

FIG. 4. Differential cross sections from Ref. [1] at 486 MeV with normalization factor 1.00. The solid line represents the fit of the present work.

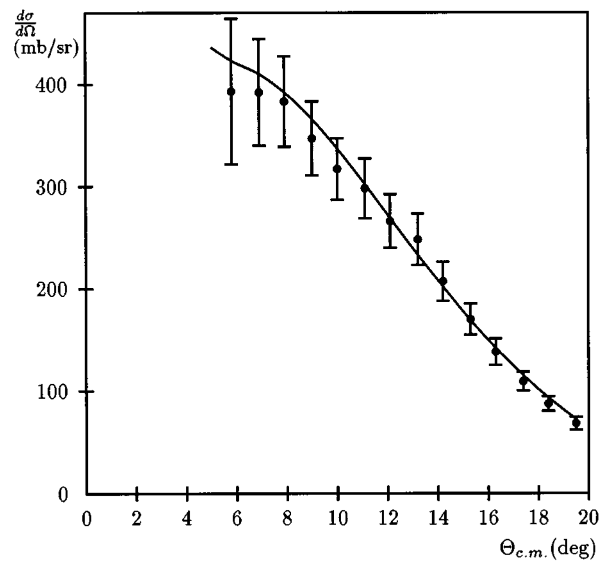

FIG. 5. Differential cross sections from Ref. [1] at 486 MeV with normalization factor 1.28. The solid line represents the fit of the present work.

Eq. (2). After a partial wave decomposition, the amplitude $f_{\mathrm{tot}}^{\pm}$ can be expressed in terms of real and imaginary phase shifts $\delta^{\pm}$ and $\omega^{\pm}$:

$$f_{\mathrm{tot},l}^{\pm}=\frac{1}{2ik}\;[e^{2i(\delta_{\mathrm{tot},l}^{\pm}+i\omega_{\mathrm{tot},l}^{\pm})}-1]. \tag{10}$$

The Coulomb corrections read in terms of these phase shifts [7]

$$\delta_{R,l}^{\pm}=\delta_{\mathrm{tot},l}^{\pm}-\delta_{h,l}-\delta_{C,l}^{\pm}, \tag{11}$$

$$\omega_{R,l}^{\pm}=\omega_{\mathrm{tot},l}^{\pm}-\omega_{h,l} \tag{12}$$

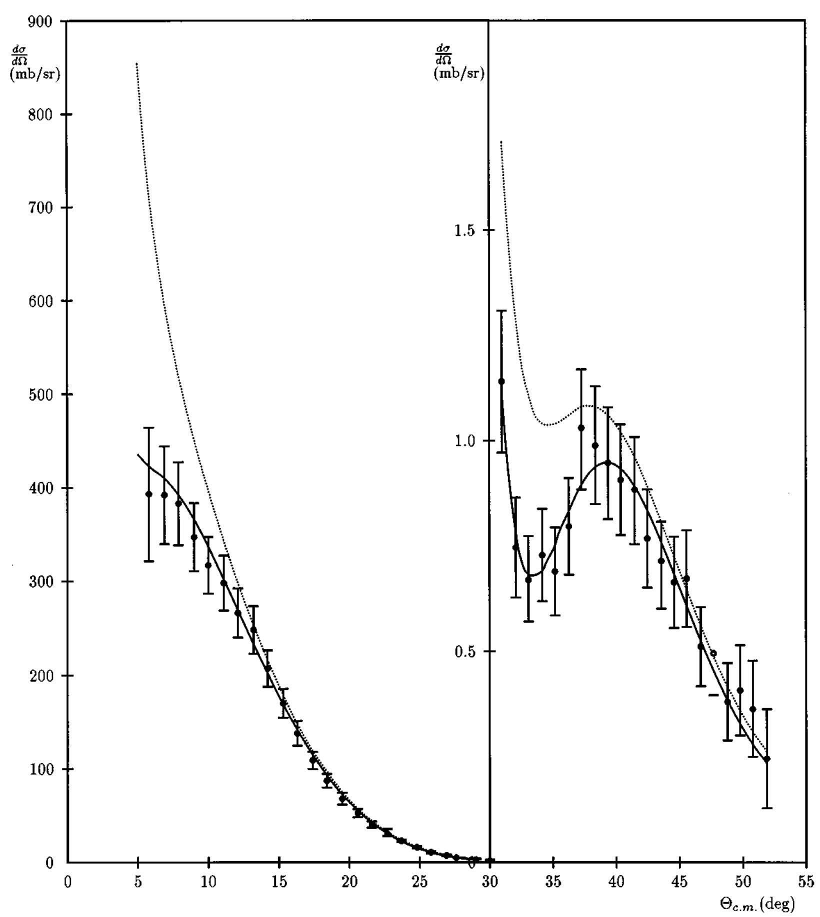

FIG. 6. Differential cross sections from Ref. [1] at 486 MeV with normalization factor 1.28. The solid line represents the fit of the present work, the dotted line stands for π^+ scattering.

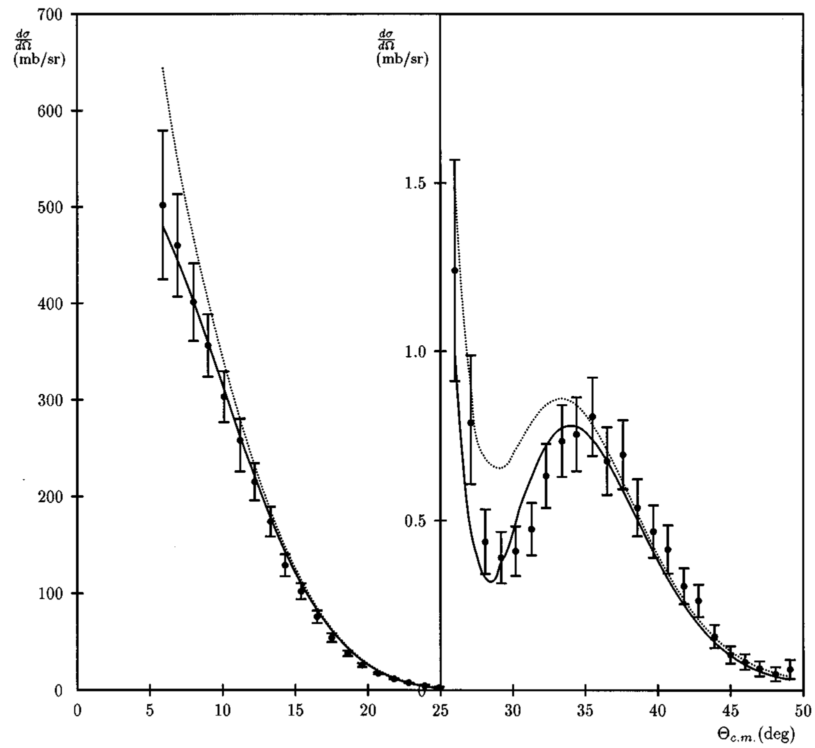

FIG. 7. Differential cross sections from Ref. [1] at 584 MeV with normalization factor 1.13. The solid line represents the fit of the present work, the dotted line stands for π^+ scattering.

with

$$\delta^{\pm}_{R,l} = \hat{\alpha}^{\pm}_l \left(\frac{d\delta_{h,l}}{dk} + \frac{1}{2k} \sin 2\delta_{h,l} \cosh 2\omega_{h,l} \right), \tag{13}$$

$$\omega^{\pm}_{R,l} = \hat{\alpha}^{\pm}_l \left(\frac{d\omega_{h,l}}{dk} + \frac{1}{2k} \cos 2\delta_{h,l} \sinh 2\omega_{h,l} \right), \tag{14}$$

and with the Coulomb factors

$$\hat{\alpha}^{\pm}_l = \pm \frac{2m_\pi Z\alpha k}{\pi} \, P\int_0^\infty dk' \, \frac{k'^2}{k^2 - k'^2} \times \int_{-1}^{1} dx \, \frac{P_l(x) F_C(q^2) F_\pi(q^2)}{q^2}, \tag{15}$$

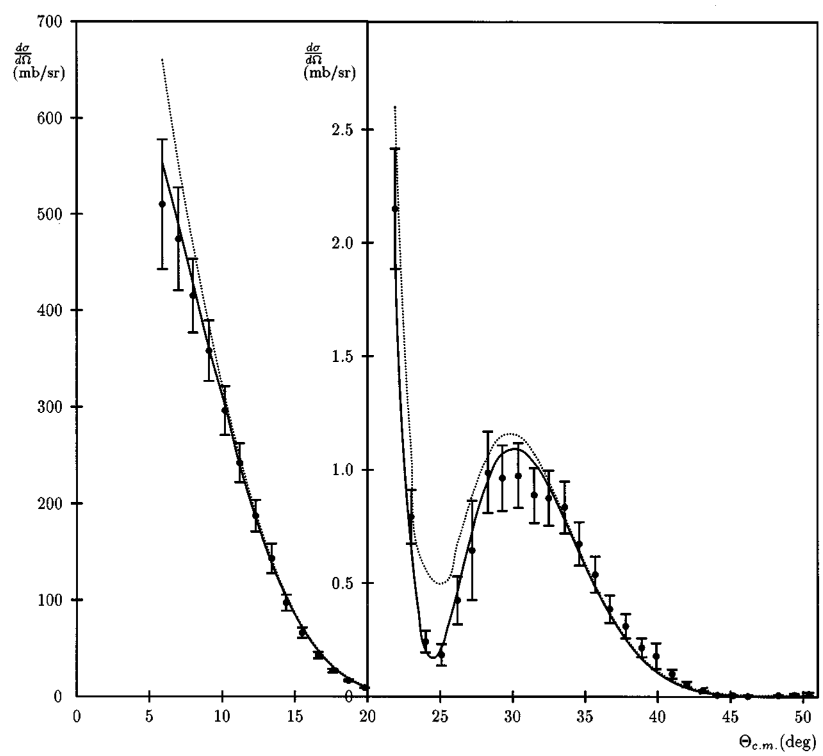

FIG. 8. Differential cross sections from Ref. [1] at 662 MeV with normalization factor 1.17. The solid line represents the fit of the present work, the dotted line stands for π^+ scattering.

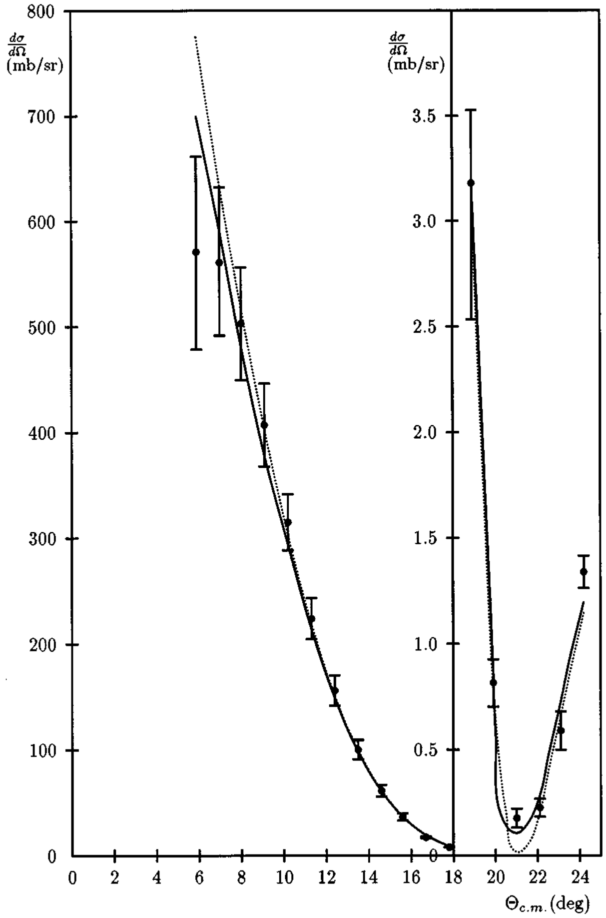

FIG. 9. Differential cross sections from Ref. [1] at 766 MeV with normalization factor 1.22. The solid line represents the fit of the present work, the dotted line stands for π^+ scattering.

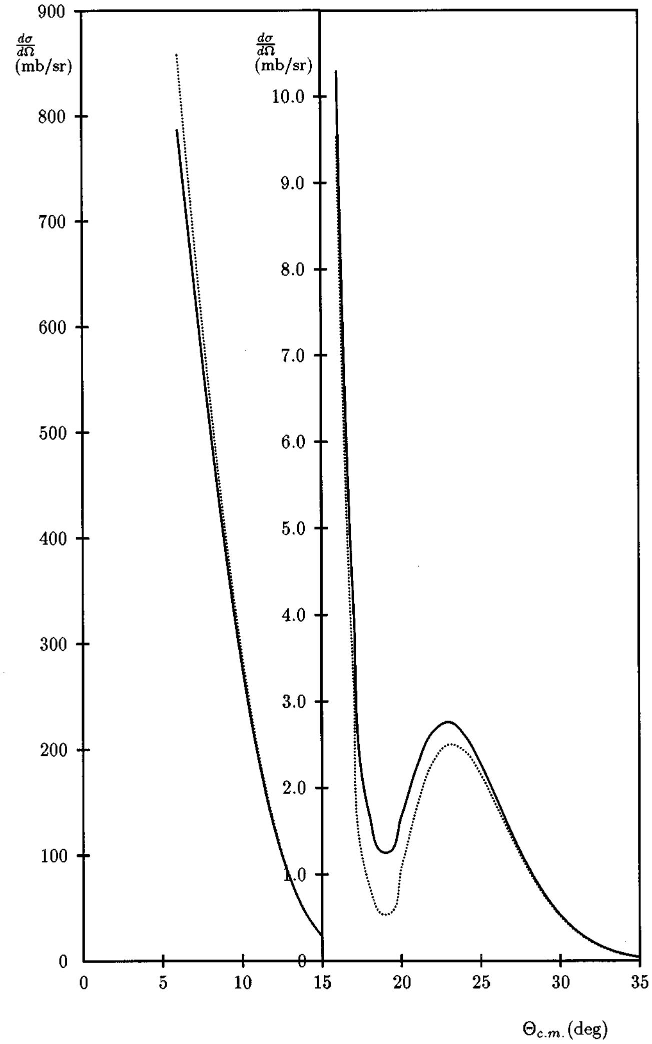

FIG. 10. Prediction of differential cross sections at 870 MeV. Parameters are extrapolated from the fit to the data of Ref. [1]. The solid line represents π^- and the dotted line stands for π^+ scattering.

where m_π is the pion mass and q is the transfered momentum. As not only the hadronic phases $\delta_{h,l}$ and $\omega_{h,l}$ but also their derivatives $d\delta_{h,l}/dk$ and $d\omega_{h,l}/dk$ are needed for the calculation of the cross section, this formalism can only be used in an energy-dependent analysis.

III. DISPERSION RELATION

For the crossing symmetric hadronic amplitude f_h the once subtracted dispersion relation reads

$$\mathrm{Re} f_h(k^2,t=0)=\mathrm{Re} f_h(m_\pi)+\sum_i \frac{2\omega_i f_i^2 k^2}{(\omega^2-\omega_i^2)k_i^2} + \frac{2k^2}{\pi} P\int_{\omega_n}^{\infty} \frac{\omega' d\omega'}{k'^2} \frac{\mathrm{Im} f_h}{\omega'^2-\omega^2}, \quad (16)$$

where $f_h(m_\pi)=A_0=(-0.451+0.132i)$ fm [16] is the complex scattering length at $T_\pi=0$ MeV, and the pole sum represents the contribution from excited nuclear states. The lower limit of the integrand is the nucleon emission threshold ω_n. For the threshold expansion of Im f_h we follow the procedure of Pilkuhn *et al.* [10] and divide it into three pieces

$$\mathrm{Im} f_h=\mathrm{Im}_{\mathrm{I}} f_h+\mathrm{Im}_{\mathrm{II}} f_h+\mathrm{Im}_{\mathrm{el}} f_h, \quad (17)$$

where $\mathrm{Im}_{\mathrm{I}} f_h$ comes from pion absorption on one nucleon, $\mathrm{Im}_{\mathrm{II}} f_h$ from two or more nucleon absorption, and $\mathrm{Im}_{\mathrm{el}} f_h$ from elastic π-nucleus scattering. As $\mathrm{Im}_{\mathrm{I}} f_h$ is negligible throughout the physical region, it is sufficient to combine the dispersion integral over it with the poles into a single effective pole $f_{\mathrm{eff}}^2/(\omega_n^2-\omega^2)$. Assuming moreover $\omega_n^2 \ll \omega^2$, $k_n^2 \approx -m_\pi^2$ we obtain

$$\mathrm{Re} f_h(k^2,t=0)=\mathrm{Re} A_0-\frac{2k^2}{m_\pi^2\omega^2}\ \omega_n f_{\mathrm{eff}}^2 + \frac{2k^2}{\pi} P\int_{2\omega_n}^{\infty} \frac{\omega' d\omega'}{k'^2} \frac{\mathrm{Im} f_h-\mathrm{Im}_{\mathrm{I}} f_h}{\omega'^2-\omega^2}, \quad (18)$$

where the lower limit for the integration is twice the ^{12}C threshold for neutron emission $\omega_n=18.3$ MeV [10]. The magnitude of the effective pole is not well determined theoretically, but its contribution to Re f_0 is believed to be small [17] or put to zero. Our best fit leads to $\omega_n f_{\mathrm{eff}}^2=-25$ MeV. This value fits nicely to the results obtained for other nuclei,

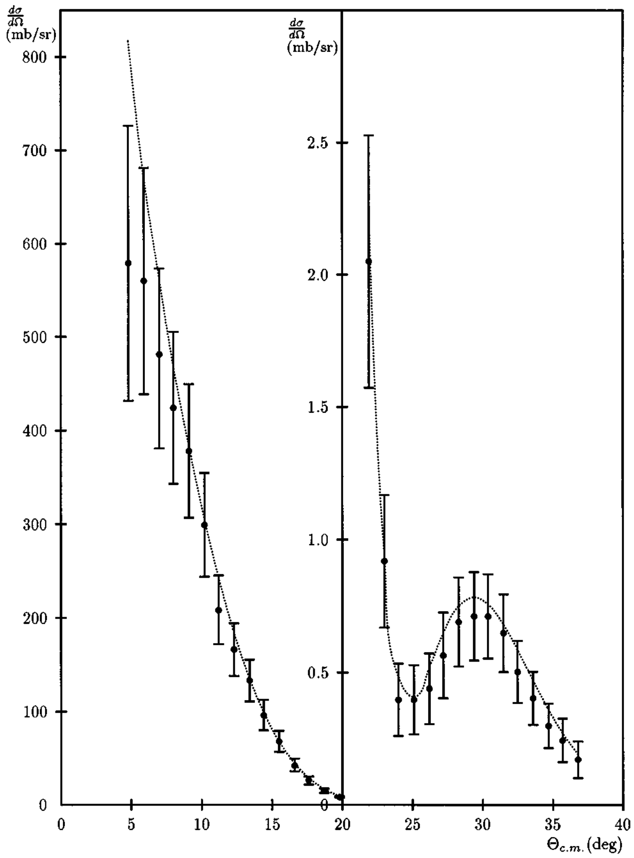

FIG. 11. Differential cross sections from Ref. [2] at 672 MeV for π^+ scattering with normalization factor 1.00. The dotted line represents the fit of the present work.

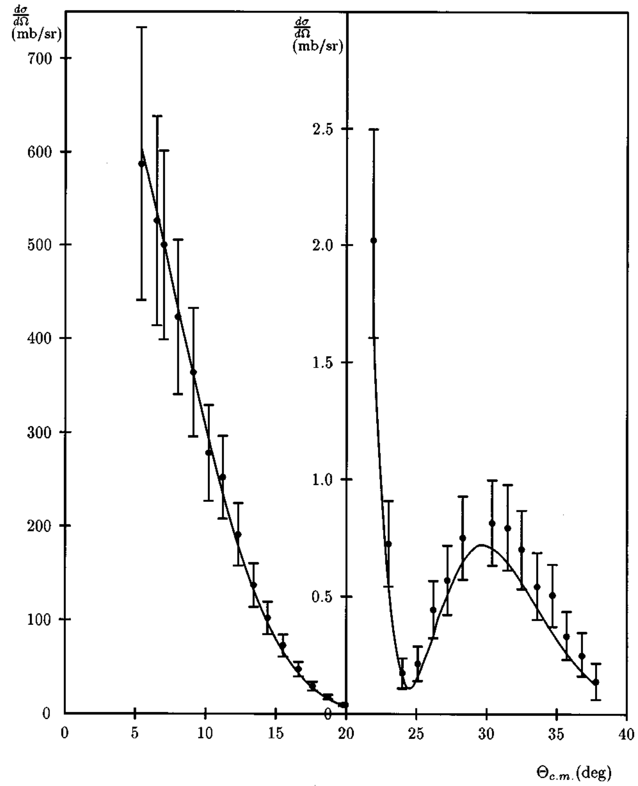

FIG. 12. Differential cross sections from Ref. [2] at 672 MeV for π^- scattering with normalization factor 1.00. The solid line represents the fit of the present work.

see Table I. Switching $\omega_n f_{\rm eff}^2$ to zero changes Re f_0 by 0.4 fm at 486 MeV which fits less well to the data of Ref. [1]. Furthermore $\omega_n f_{\rm eff}^2$ must be about -25 MeV to reach the maximum of Re f_0 at 80 MeV. For a better determination of the effective coupling constant, more accurate differential cross sections at small angles for $\pi^{\pm}$ scattering should be taken. To estimate the contribution of the integral close to threshold we use the threshold expansion [10]

$$f_{\rm threxp}=\frac{A_0+k^2B_0}{1-ik(A_0+k^2B_0)}+\frac{3k^2}{1/A_1-ik^3} \tag{19}$$

with

$$B_0=-0.49\ \ {\rm fm}^3,$$

$$A_1=(1.54+0.34i)\ \ {\rm fm}^3.$$

Because the dominating contribution to the scattering amplitude at threshold comes from two-nucleon absorption, we multiply $f_{\rm threxp}$ with the approximate phase space factor for this reaction to obtain

$${\rm Im}f_h-{\rm Im}_{\rm I}f_h=\frac{\omega-2\omega_n}{m_\pi-2\omega_n}\,{\rm Im}f_{\rm threxp}. \tag{20}$$

This threshold expansion is used up to an energy of $T_\pi=20$ MeV where inelastic π-^{12}C scattering starts to contribute.

TABLE II. Fit parameters: f_0 is the forward amplitude as gained by forward dispersion relation, B is the slope parameter, t_1 and t_2 are the two complex zeros, and N is the normalization factor for the differential cross sections.

T_π (MeV)	f_0 (fm)	B (GeV/c)^2	t_1 (GeV/c)$^{-2}$	t_2 (GeV/c)$^{-2}$	N	Reference
486	$-3.11+7.15i$	13.25	$-0.102+0.024i$	$-0.280+0.120i$	1.28	[1]
584	$-2.34+7.85i$	13.87	$-0.102+0.017i$	$-0.318+0.084i$	1.13	[1]
662	$-1.84+8.70i$	14.26	$-0.097+0.011i$	$-0.340+0.037i$	1.17	[1]
672	$-1.76+8.90i$	15.30	$-0.099+0.011i$	$-0.341+0.037i$	1.00	[2]
766	$-1.53+10.30i$	14.99	$-0.093-0.002i$	$-0.362-0.011i$	1.22	[1]
870	$-1.64+11.70i$	15.60	$-0.088-0.011i$	$-0.386-0.035i$	1.00	Present work

TABLE III. Total elastic, total inelastic, and total cross sections from the analysis. The experimental results are from Refs. [1] to [3].

T_π (MeV)	$\sigma_{\rm el}$ (mb)	$\sigma_{\rm inel}$ (mb)	$\sigma_{\rm tot}$ (mb)	$\sigma_{\rm tot}$ (exp.)	Reference
486	105	201	306	270.8 ± 8.6	[1]
584	83	208	291	272.5 ± 8.9	[1]
662	77	215	292	294.2 ± 8.9	[1]
672	76	219	295	296.3 ± 10.0	[2]
766	80	228	308	316.4 ± 11.4	[1]
870	82	232	314	317.0 ± 9.0	[3]

IV. THE HADRONIC AMPLITUDE

The general features of the angular distribution of the differential cross sections of π-^{12}C scattering from 486 to 870 MeV are well described by the following parametrization [6]:

$$f_h(k,t)=f_0(k)e^{B(k)t}\prod_{i=1}^{2}\left[1-t/t_i(k)\right] \tag{21}$$

with $t=-2k^2(1-\cos\Theta)$, where k and Θ are the c.m. momentum and scattering angle, respectively. The ansatz includes the forward amplitude f_0, the exponential slope expressed by B, a real function of k, and two complex functions of k, the t_i's, which describe the cross section near the first and possible second minimum. To be able to use this ansatz together with the Coulomb corrections described in Sec. II, a Legendre polynomial decomposition of the hadronic amplitude is made to obtain the hadronic phases. The imaginary part of the forward amplitude arises from total cross sections by the optical theorem: Im $f_0=(k/4\pi)\sigma^{\rm tot}$. The real part of the forward amplitude is gained by dispersion relation, see Sec. III, thus the forward amplitude is a reliable input within the calculation, as the values of the hadronic amplitude are fixed at $\Theta=0$. The hadronic amplitude interferes with the known Coulomb amplitude and in this way the data are forced to have the right order of normalization. Taking into account the forward dispersion relation and the fact, that the shape of the real part of f_0 over the energy has no free parameters besides the effective coupling constant, the normalization of the data can be checked. (A normalization factor in front of the forward amplitude would only reflect an incorrect normalization of the data). As the measured data are a mixture of strong and Coulomb interaction, we prefer to renormalize the data themselves, as the hadronic part for itself cannot be measured separately. The ansatz (21) allows a simple inclusion of the forward amplitude f_0 therefore the constraints given by dispersion relation and unitarity are satisfied. The expression for Im f_0 is a smooth interpolation of the old data [10] up to 1300 MeV, but cannot meet the Im f_0 extracted from Ref. [1] at 486 and 584 MeV which are about 15% too low. For energies greater than 1300 MeV the asymptotic parametrization [17,23]

$$\sigma^{\rm tot}=\sigma^{\infty}+\sqrt{\frac{B_a}{\omega}} \tag{22}$$

is used with $\sigma^{\infty}=0.20$ b and $B_a=25.70$ MeV b^2. This formula reproduces well the earlier total cross sections, but not the total cross sections extracted from Ref. [1], One has two possibilities:

(1) To rely on the earlier total cross sections; then the forward amplitude runs about 10–15% above the data of Takahashi *et al.* and one has to use normalization factors to meet the new differential cross sections.

(2) To force the forward amplitude down to the region required by Takahashi *et al.* But then the earlier measured total cross sections cannot be met from 350 to 1000 MeV. At 486 and 584 MeV the total cross sections quoted by Takahashi et al agree with those extracted from their differential cross sections, but at 662 and 776 MeV the total cross sections extracted from their differential cross sections lie significantly below their quoted total cross sections. Total cross sections along the dotted line in Fig. 1 allow a represention of the differential cross sections of Takahashi *et al.* [1] without normalization factors. But now we have a broad deviation from all earlier total cross sections from 300 to 1000 MeV which seems unlikely to us.

Therefore we decided to rely on the whole set of old total cross sections and use normalization factors for the differential cross sections of Takahashi *et al.* Accurate measurements of total cross sections as well as differential cross sections for both π^- and π^+-^{12} C scattering at small angles in the energy range from 300 to 1000 MeV would be helpful to give a better determination of the forward amplitude. Due to the large systematic errors quoted by Ref. [1] an analysis of their data at small angles leads to large error bars for the forward amplitude. This way the data are compatible with the old forward dispersion relation. The differential cross sections of Ref. [1] can be well described by our ansatz. The predicted π^+ data show pronounced differences compared with the measured π^- data, they lie significantly above the π^- data in the near forward region as well as in the first minimum up to 750 MeV where the situation changes as indicated by a change of sign in Imt_1, the generator of the first minimum.

V. DISCUSSION OF RESULTS AND CONCLUSIONS

Figure 1 presents the measured total cross sections together with our interpolation. The values at $T_\pi=486$ and 584 MeV taken from Ref. [1] are clearly below the other data in this region, therefore we did not include them. It seems important to us that new measurements of the total cross sections are taken from 300 to 1000 MeV in order to fix the

TABLE IV. Reconstructed phases from the analysis of π^0-^{12}C scattering.

δ_l / T_π (MeV)	486	584	662	672	766	870
0	−34.066	−21.649	−10.837	−11.284	−13.950	−18.129
1	−33.991	−20.407	−10.756	−11.150	−14.013	−18.153
2	−32.875	−18.593	−10.760	−10.936	−14.004	−18.078
3	−28.754	−16.788	−10.843	−10.597	−13.658	−17.665
4	−22.385	−14.782	−10.637	−9.942	−12.676	−16.596
5	−15.927	−12.255	−9.743	−8.834	−10.936	−14.626
6	−10.490	−9.434	−8.187	−7.369	−8.681	−11.831
7	−6.420	−6.768	−6.350	−5.789	−6.393	−8.719
8	−3.649	−4.557	−4.613	−4.316	−4.454	−5.921
9	−1.920	−2.891	−3.176	−3.072	−2.991	−3.784
10	−0.930	−1.728	−2.085	−2.096	−1.958	−2.317
11	−0.414	−0.971	−1.306	−1.371	−1.254	−1.374
12	−0.169	−0.511	−0.780	−0.858	−0.787	−0.791
13	−0.064	−0.252	−0.443	−0.513	−0.482	−0.442
14	−0.022	−0.116	−0.239	−0.292	−0.287	−0.238
15	−0.007	−0.050	−0.122	−0.159	−0.165	−0.122
16	−0.002	−0.020	−0.059	−0.082	−0.092	−0.059
17	−0.001	−0.008	−0.027	−0.040	−0.049	−0.027
18	−0.000	−0.003	−0.012	−0.019	−0.026	−0.010
19	−0.000	−0.001	−0.005	−0.008	−0.013	−0.003
20	−0.000	−0.000	−0.002	−0.004	−0.006	0.000
η_l / T_π (MeV)	486	584	662	672	766	870
0	0.272	0.212	0.230	0.205	0.272	0.359
1	0.239	0.210	0.234	0.212	0.271	0.352
2	0.222	0.217	0.243	0.227	0.270	0.341
3	0.258	0.246	0.261	0.252	0.273	0.327
4	0.352	0.303	0.295	0.293	0.284	0.316
5	0.484	0.389	0.348	0.350	0.307	0.314
6	0.628	0.497	0.423	0.425	0.349	0.326
7	0.759	0.615	0.515	0.515	0.411	0.358
8	0.860	0.728	0.617	0.611	0.490	0.411
9	0.927	0.822	0.717	0.705	0.580	0.480
10	0.966	0.893	0.804	0.790	0.671	0.560
11	0.985	0.940	0.873	0.859	0.756	0.643
12	0.994	0.969	0.923	0.910	0.828	0.722
13	0.998	0.985	0.956	0.946	0.885	0.792
14	0.999	0.993	0.977	0.970	0.927	0.851
15	1.000	0.997	0.988	0.984	0.955	0.897
16	1.000	0.999	0.994	0.992	0.974	0.932
17	1.000	1.000	0.997	0.996	0.986	0.956
18	1.000	1.000	0.999	0.998	0.993	0.973
19	1.000	1.000	1.000	0.999	0.996	0.984
20	1.000	1.000	1.000	1.000	0.998	0.991

shape of the forward amplitude. Figure 2 shows the imaginary part of the forward amplitude as gained from the total cross sections presented in Fig. 1. Figure 3 presents the real part of the forward amplitude as calculated by dispersion relation. For energies about 100 MeV the calculated real part does not meet the real parts taken from the quoted earlier experiments. The Coulomb effects in this region are strong and new precise measurements of $\pi^{\pm}$ differential cross sections are needed. The effective coupling is chosen to meet best the real parts of the forward amplitude from $T_\pi = 150-350$ MeV. In such cases where the experiments did not provide real parts the ratio of real to imaginary parts from Wilkin [18] has been adopted. Figure 4 shows an attempt to fit the data at 486 MeV from Ref. [1] without normalization factor. A factor of 1.28 as shown in Fig. 5 is needed for a good fit. We present our fits to the data of Ref. [1] in Figs. 6–9, where the dotted line is our prediction for the still not measured π^+-^{12}C elastic differential cross sections. Due to the large systematic errors, the disagreement between theory and experiment [5] at 790 MeV/c is practically removed by the datasets of Ref. [1]. In Fig. 10 we present our predictions at 870 MeV. In Figs. 11 and 12 we show our fit together with the data of Ref. [2]. Here, no normalization of the differential cross sections is needed, but the slope parameter is about 7% larger compared with the slopes extracted from the data of Ref. [1]. A few precise measurements of the differential cross section of $\pi^{\pm}$-^{12}C at small angles would be extremely helpful to get the forward amplitude. The datasets of Takahashi *et al.* [1] and Marlow *et al.* [2] are compatible only due to the large systematic errors quoted. The parameters of the fits are gathered in Table II. Table III presents the total elastic and total inelastic cross sections. In Table IV we give the purely hadronic phase shifts δ_l^0 and the inelasticity parameters η_l^0 for the π^0-^{12}C elastic scattering from 486 to 870 MeV.

In conclusion, using an amplitude analysis that contains a careful treatment of Coulomb effects and the forward dispersion relation we can show that the data of Ref. [1] fit into this framework, provided normalization factors up to 1.28 are used. Additional measurements of the total cross sections from 300 to 1000 MeV would be very helpful for a better determination of the forward amplitude including the effective coupling constant. A few accurate measurements of the differential cross sections at small angles, smaller than 10°, would show how consistent the differential cross sections are with the total cross sections.

ACKNOWLEDGMENTS

The author wishes to thank V. Hund and H. Pilkuhn for helpful discussions.

[1] T. Takahashi, H. Sakaguchi, K. Aoki, T. Hasegawa, O. Hashimoto, T. Nagae, M. Sekimoto, A. Ohkusu, H. Bhang, H. Yu, and Y. Gavrilov, Phys. Rev. C **51**, 2542 (1995).

[2] D. Marlow, P. D. Barnes, N. J. Colella, S. A. Dytman, R. A. Eisenstein, R. Grace, P. Pile, F. Takeutchi, W. R. Wharton, S. Bart, D. Hancock, R. Hackenberg, E. Hungerford, W. Mayes, L. Pinsky, T. Williams, R. Chrien, H. Palevsky, and R. Sutter, Phys. Rev. C **30**, 1662 (1984).

[3] M. Crozon, Ph. Chavanon, A. Courau, Th. Leray, J. L. Narjoux, and J. Tocqueville, Nucl. Phys. **64**, 567 (1965).

[4] A. S. Clough, G. K. Turner, B. W. Allardyce, C. J. Batty, D. J. Baugh, W. J. McDonald, R. A. J. Riddle, L. H. Watson, M. E. Cage, G. J. Pyle, and G. T. A. Squier, Nucl. Phys. **B76**, 15 (1974).

[5] Victor Franco and H. G. Schlaile, Phys. Rev. C **41**, 1075 (1990).

[6] B. Brinkmöller and H. G. Schlaile, Phys. Rev. C **48**, 1973 (1993).

[7] O. Dumbrajs, J. Fröhlich, U. Klein, and H. G. Schlaile, Phys. Rev. C **29**, 581 (1984).

[8] J. Fröhlich, H. G. Schlaile, L. Streit, and H. Zingl, Z. Phys. A **302**, 89 (1981).

[9] J. Fröhlich, H. Pilkuhn, and H. G. Schlaile, Nucl. Phys. **A415**, 399 (1984).

[10] H. Pilkuhn, N. Zovko, and H. G. Schlaile, Z. Phys. A **279**, 283 (1976).

[11] J. Fröhlich, I. Streit, H. Zankel, and H. Zingl, J. Phys. G **6**, 841 (1980).

[12] O. Dumbrajs, Z. Phys. A **301**, 55 (1981).

[13] C. J. Bebek, C. N. Brown, S. D. Holmes, R. V. Kline, F. M. Pipkin, S. Raither, L. K. Sisterson, A. Browman, K. M. Hanson, D. Larson, and A. Silverman, Phys. Rev. D **17**, 1693 (1978).

[14] J. Fröhlich, H. Pilkuhn, and H. G. Schlaile, Phys. Lett. **121B**, 235 (1983).

[15] H. Pilkuhn, *Relativistic Particle Physics* (Springer, Berlin, 1979).

[16] J. Hüfner, L. Tauscher, and C. Wilkin, Nucl. Phys. **A231**, 455 (1974).

[17] C. J. Batty, G. T. A. Squier, and G. K. Turner, Nucl. Phys. **B67**, 492 (1973).

[18] C. Wilkin, C. R. Cox, J. J. Domingo, K. Gabathuler, E. Pedroni, J. Rohlin, P. Schwaller, and N. W. Tanner, Nucl. Phys. **B62**, 61 (1973).

[19] G. S. Mutchler, M. L. Scott, C. R. Fletcher, E. V. Hungerford, L. V. Coulson, N. D. Gabitzsch, G. C. Phillips, B. W. Mayes, L. Y. Lee, J. C. Allred, and Clark Goodman, Phys. Rev. C **9**, 1198 (1974).

[20] F. Binon, P. Duteil, J. P. Garron, J. Gorres, L. Hugon, J. P. Peigneux, C. Schmit, M. Spighel, and J. P. Stroot, Nucl. Phys. **B17**, 168 (1970).

[21] K. M. Das and B. B. Deo, Phys. Rev. C **26**, 2678 (1982).

[22] D. Ashery, I. Navon, G. Azuelos, H. K. Walter, H. J. Pfeiffer, and F. W. Schlepütz, Phys. Rev. C **23**, 2173 (1981).

[23] T. E. O. Ericson and M. P. Locher, Nucl. Phys. **A148**, 1 (1970).